

Complete dissociation of the HIV-1 gp41 ectodomain and membrane proximal regions upon phospholipid binding

Julien Roche¹, John M. Louis¹, Annie Aniana¹, Rodolfo Ghirlando² and Ad Bax¹

¹Laboratory of Chemical Physics and ²Laboratory of Molecular Biology, National Institute of Diabetes and Digestive and Kidney Diseases, National Institutes of Health, Bethesda, Maryland 20892, USA

SUPPORTING INFORMATION

SI Materials and Methods

Circular Dichroism. CD spectra were recorded at 310 K in 50 mM sodium acetate buffer at pH 4.0 on a JASCO J-810 spectropolarimeter using a 0.01 cm path length cell. The CD spectra of Core^{S 35-144} and Core^{S 17-172} were recorded at a protein concentration of 15 μ M with 10 mM DPC. Alpha-helical content was determined using the CDNN program (Bohm et al. 1992).

Sedimentation velocity. Sedimentation velocity experiments were conducted at 50,000 rpm and 20°C on a Beckman Coulter ProteomeLab XL-I analytical ultracentrifuge following standard protocols (Zhao et al. 2013). Samples of Core^{S 35-144}, Core^{1L 35-144} and Core^{S 17-172} in 50 mM sodium acetate, pH 4 with and without DPC (as described in Table S1) were loaded in 2-channel centerpiece cells and scans were collected using both the absorbance (280 nm) and Rayleigh interference (655 nm) optical detection systems. High concentration samples were loaded into 3 mm path-length cells, whereas low concentration samples were loaded into standard 12 mm path-length cells. In all cases a DPC free matching buffer was used as a reference. Sedimentation data were time-corrected (Ghirlando et al. 2013) and analyzed in SEDFIT 14.4f (Schuck 2000) in terms of a continuous $c(s)$ distribution of Lamm equation solutions with a resolution of 0.05 S and a maximum entropy regularization confidence level of 0.68. To account for the presence of the DPC detergent, interference data collected in the presence of DPC were analyzed in terms of a single species representing the detergent micelle and a non-overlapping continuous $c(s)$ distribution. In all cases, excellent fits were obtained with best-fit absorbance and interference rmsd. values ranging from 0.0034 – 0.0060 A_{280} and 0.0028 – 0.014 fringes. Solution densities ρ and viscosities η were calculated in SEDNTERP (Cole et al. 2008) (<http://sednterp.unh.edu/>). The protein partial specific volume v and absorbance extinction coefficient (ϵ_{280}) were calculated in SEDNTERP based on the amino acid composition. The partial specific volume was corrected for the ²H, ¹⁵N and ¹³C isotopic composition. The interference signal increment (ϵ_j) for the protein was calculated in SEDFIT 14.4f based on the amino acid composition (Zhao et al. 2011). A partial specific volume of 0.937 cm³g⁻¹ was used for DPC (le Maire et al. 2000), and the corresponding interference signal increment (ϵ_j) of 750 fringes M⁻¹cm⁻¹ was based on a refractive index increment (dn/dc) of 0.1398 cm³g⁻¹ (<https://www.anatrace.com/Products/Lipids/FOS-CHOLINE/F308.aspx>). Sedimentation coefficients s were corrected to $s_{20,w}$ using partial specific volumes based on the complex protein:detergent stoichiometry. The experimental protein:detergent stoichiometry was based on the integrated absorbance (protein alone) and interference (protein and detergent) signal for the major species observed in the $c(s)$ distribution (Inagaki et al. 2013). This stoichiometry was used to calculate the partial specific volume of the sedimenting protein-detergent complex and subsequently to derive its molar mass.

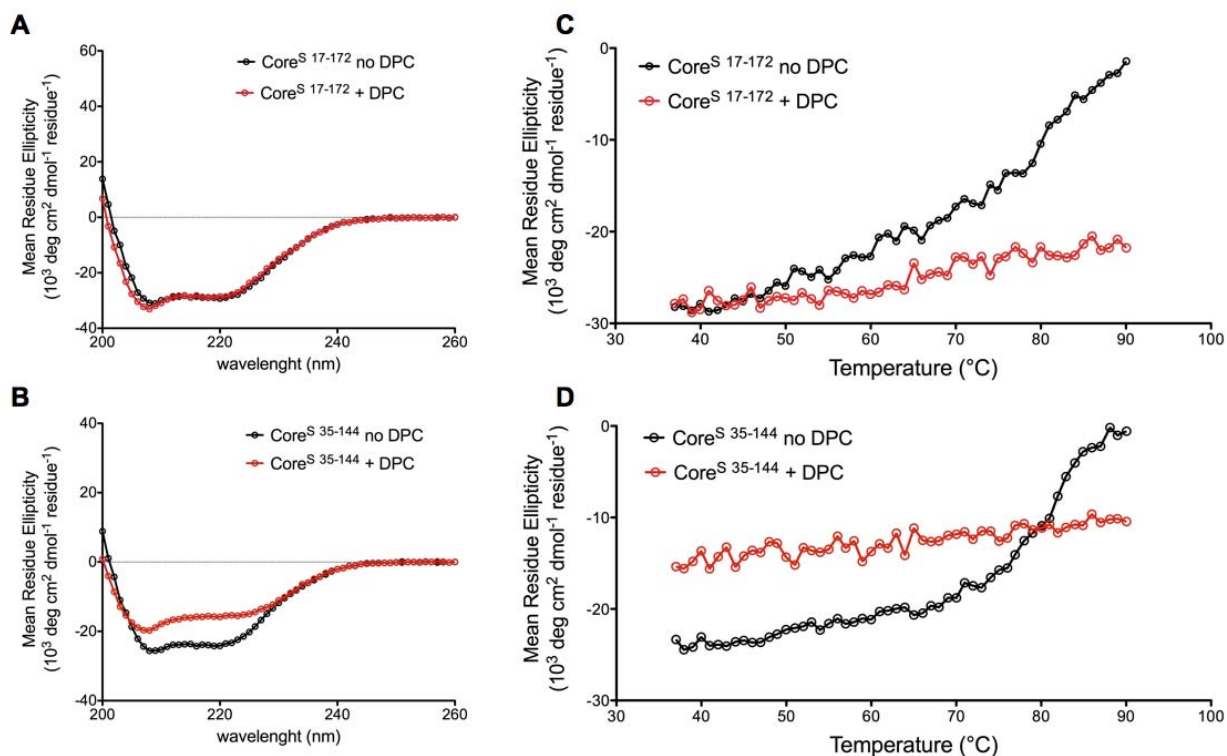


Figure S1: Secondary structure and thermostability of the ectodomain constructs. CD spectra of (A) Core^S 17-172 and (B) Core^S 35-144 recorded at 37°C in the absence of detergent (black) and in the presence of 10 mM DPC (red). Mean residue ellipticity measured at 222 nm between 37°C and 90°C for (C) Core^S 17-172 and (D) Core^S 35-144 in the absence of detergent (black) and in the presence of 10 mM DPC (red).

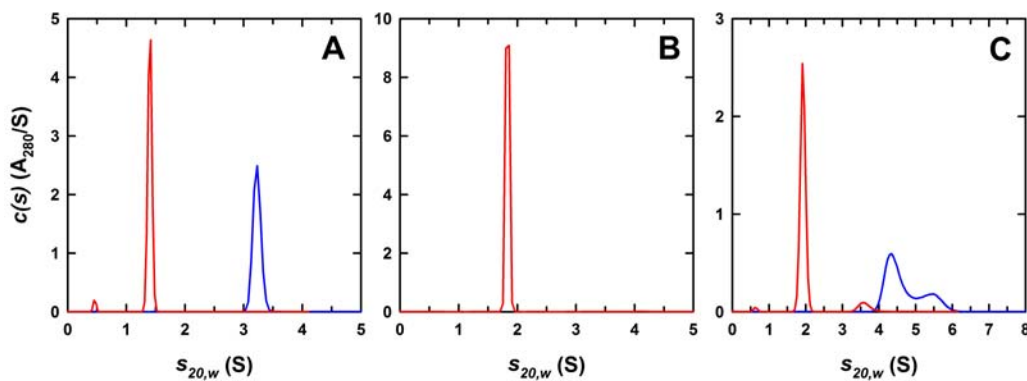


Figure S2: Sedimentation velocity absorbance $c(s)$ distributions for (A) Core^S 35-144, (B) Core^{IL} 35-144 and (C) Core^S 17-172 in the absence of DPC (blue curves) and presence of at least one molar equivalent of DPC micelles (red curve). (A) Distributions for 22 μ M Core^S 35-144 (blue) and 22 μ M Core^S 35-144 with 10 mM DPC (red), (B) Distribution for 22 μ M Core^{IL} 35-144 with 10 mM DPC (red) and (C) Distributions for 10 μ M Core^S 17-172 (blue) and 10 μ M Core^S 17-172 with 10 mM DPC (red). Similar profiles were observed using the interference optics, except for the presence of free DPC micelles when detergent was added.

Table S1. Summary of the sedimentation velocity experiments carried out on various constructs

Construct	Protein (μM)	DPC (mM)	protein:micelle ratio	$M_{\text{experimental}}$ (kDa) (Sedimentation coefficient (S))	$M_{\text{calculated}}$ (kDa)	Major species
Core ^{S 35-144}	10	-	-	32.1 ± 2.0 (3.22 ± 0.02 S)	9166	trimer
Core ^{S 35-144}	10	2.15	1:1	31.4 ± 2.9 (1.42 ± 0.03 S)	9166	monomer + 55 DPC
Core ^{S 35-144}	22	-	-	29.2 ± 0.8 (3.24 ± 0.01 S)	9166	trimer
Core ^{S 35-144}	110	-	-	28.7 ± 0.1 (3.12 ± 0.01 S) ^a	9166	trimer
Core ^{S 35-144}	22	10	1:6	30.4 ± 2.4 (1.42 ± 0.02 S)	9166	monomer + 55 DPC
DPC	-	10	-	24.2 (0.55 S) ^b	352	69 DPC
Core ^{IL 35-144}	22	10	1:6	40.4 ± 1.2 (1.84 ± 0.01 S)	16585	monomer + 63 DPC
Core ^{S 17-172}	10	-	-	$46.5 / 63.0$ ($4.44 / 5.44$ S) ^c	14825	trimer/tetramer
Core ^{S 17-172}	10	10	1:13	40.5 ± 2.6 (1.94 ± 0.01 S)	14825	monomer + 73 DPC

- (a) Due to the higher loading concentration, a slightly smaller sedimentation coefficient is determined reflecting repulsive non-ideality.
- (b) A partial specific volume of 0.937 mL/g was used for DPC in these studies.
- (c) The $c(s)$ distribution showed the presence of two sedimenting species, simply interpreted in terms of a mixture of trimers and tetramers. As data were only collected at a single concentration, a reversible trimer to higher order aggregate self-association cannot be ruled out. In such a case, and in the presence of fast exchange kinetics, the faster sedimenting species would represent a reaction boundary.

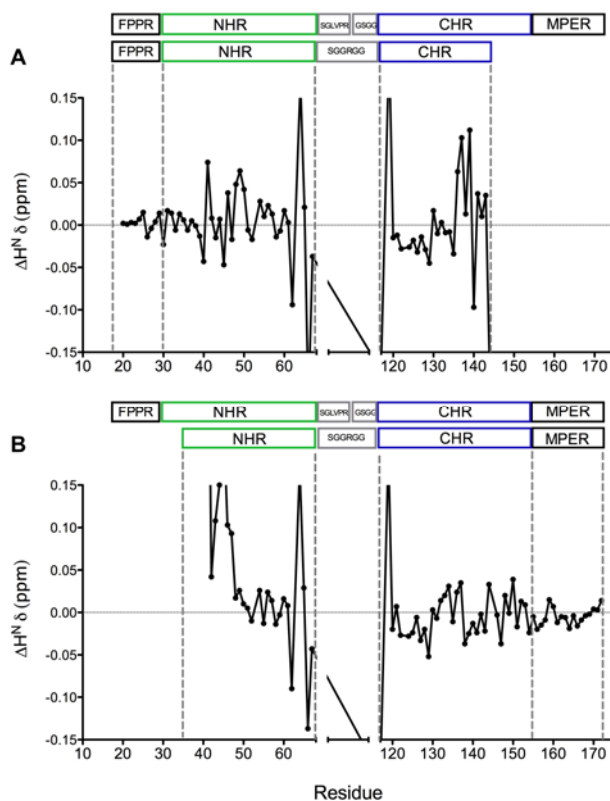


Figure S3: Comparison of the backbone chemical shifts recorded for $Core^S_{17-144}$, $Core^S_{35-172}$ and $Core^{SP}_{17-172}$ in 25 mM sodium phosphate (pH 6.0) in the presence of 100 mM DPC. The length of each region (FPPR, NHR, CHR and MPER), is depicted at the top of each panel (see Material and Methods for details about the $Core^{SP}_{17-172}$ construct). (A) Backbone amide proton chemical shifts difference between $Core^S_{17-144}$ and $Core^{SP}_{17-172}$. (B) Backbone amide proton chemical shifts difference between $Core^S_{35-172}$ and $Core^{SP}_{17-172}$. Note that the NHR and CHR helices of $Core^{SP}_{17-172}$ each extend by three additional residues towards IL, and also contain several terminal residues resulting from the thrombin cleavage site (See Fig. 2F, main text).

H643	117.81	8.323	59.11	117.82	8.345	59.07	117.84	8.322	59.14	117.91	8.245	117.86	8.248	117.81	8.259
S644	115.38	8.134	61.65	115.34	8.146	61.59	115.41	8.135	61.66	114.95	8.076	114.90	8.067	115.06	8.096
L645	122.57	7.920	57.35	122.48	7.918	57.26	122.62	7.923	57.40	122.08	7.809	121.93	7.801	122.16	7.840
I646	118.13	7.931	63.94	117.93	7.925	63.80	118.24	7.941	64.02	116.20	7.752	116.34	7.718	116.30	7.741
E647	119.53	7.873	57.46	119.59	7.912	57.49	119.49	7.868	57.55	121.40	7.867	121.37	7.930	121.36	7.891
E648	119.30	8.012	56.95	119.03	8.057	57.03	119.07	7.965	56.96	120.31	8.087	120.40	8.190	120.37	8.122
S649	115.44	7.932	59.55	115.30	7.909	59.57	115.40	7.928	59.61	116.03	7.991	116.06	8.004	116.08	7.954
Q650	120.84	7.953	56.61	120.49	7.843	55.78	120.79	7.944	56.71	120.40	7.981	121.03	8.093	120.49	7.956
N651	118.13	8.025	53.75	119.23	8.080	53.26	118.23	8.047	53.81	119.84	8.157	119.41	8.060	119.73	8.144
Q652	120.61	8.057	56.41	120.79	8.165	55.70	120.46	8.045	56.35	120.63	8.145	121.11	8.182	120.59	8.121
Q653	120.29	8.224	57.05	121.15	8.222	55.61	120.19	8.230	57.14	121.09	8.200	121.46	8.210	121.03	8.198
E654	119.90	8.128	57.03	122.36	8.210	55.62	119.92	8.147	57.05	121.78	8.258	123.13	8.293	121.69	8.236
K655	121.28	8.010	57.30	126.99	7.904	56.74	121.18	7.982	57.23	120.54	7.977	127.89	7.802	120.56	8.010
N656			54.08						54.02						
E657	120.54	8.224	57.92				120.49	8.237	58.00	121.55	8.384			121.44	8.381
Q658	119.25	8.179	58.04				119.11	8.164	58.03	120.12	8.206			120.02	8.169
E659	119.56	8.066	58.02				119.46	8.051	57.99	121.28	8.113			121.22	8.133
L660	119.94	7.890	57.11				119.87	7.882	57.09	119.84	7.935			119.78	7.934
L661	118.75	7.800	56.73				118.65	7.769	56.63	118.29	7.750			118.38	7.789
E662	119.15	7.779	57.41				119.07	7.759	57.27	118.59	7.941			118.65	7.924
L663	120.72	7.971	57.33				120.85	7.978	57.33	121.07	7.961			121.04	7.974
D664	117.16	8.241	55.55				117.19	8.256	55.63	119.09	8.358			118.99	8.367
K665	120.05	7.796	58.01				119.98	7.781	57.96	121.30	7.942			121.37	7.918
W666	120.84	7.865	58.58				120.87	7.845	58.54	120.46	7.771			120.42	7.766
A667	121.26	8.130	54.31				121.29	8.122	54.32	121.34	8.100			121.37	8.080
S668	112.52	7.850	60.30				112.51	7.842	60.29	113.06	7.983			113.08	7.968
L669	122.23	7.625	56.42				122.24	7.610	56.41	123.04	7.716			123.00	7.707
W670	118.86	7.629	57.70				118.82	7.607	57.75	118.51	7.887			118.54	7.902
N671	117.54	7.961	53.84				117.57	7.959	53.85	116.37	7.963			116.48	7.970
W672	121.26	8.056	59.05				121.23	8.024	59.03	121.82	8.108			121.86	8.096
F673	118.27	7.847	58.80				118.19	7.823	58.72	117.97	7.838			118.07	7.833
N674	118.51	7.784	53.58				118.51	7.763	53.49	118.25	7.691			118.33	7.685
I675	119.90	7.910	63.14				119.95	7.912	63.13	119.86	7.947			119.86	7.928
T676	113.79	7.884	65.02				113.90	7.864	65.01	114.69	7.811			114.60	7.807
N677	119.50	7.760	54.85				119.51	7.763	54.72	119.46	7.786			119.44	7.770
W678	119.74	7.724	58.69				119.74	7.714	58.64	119.73	7.709			119.70	7.700
L679	118.33	7.786	56.64				118.33	7.747	56.55	118.26	7.764			118.25	7.760
W680	117.53	7.577	58.69				117.61	7.539	58.61	117.92	7.470			117.89	7.468
Y681	116.73	7.436	59.29				116.82	7.419	59.25	116.70	7.389			116.75	7.393
I682	115.99	7.416	60.93				116.05	7.405	60.86	115.59	7.400			115.65	7.403
K683	123.65	7.404	56.06				124.77	7.389	56.26	127.48	7.296			127.56	7.310

^a Chemical shifts are in ppm relative to DSS (¹H, ¹³C) and liquid ammonia (¹⁵N). Residue numbering follows that of full-length gp41 (see Fig 2, main text). The six residues replacing the immunodominant loop (I69-T116) in the Core^S constructs are numbered loopS1-loopG6.

Table S3: ^{15}N relaxation rates R_1 and R_2 and heteronuclear $^{15}\text{N}-\{^1\text{H}\}$ NOE measured at 600 MHz in the presence of 100 mM DPC for Core^{S 17-172}, Core^{S 17-144} and Core^{S 35-172} in 50 mM sodium acetate pH 4.0, at 310 K.

	17-172 R_1 (s^{-1}) 600 MHz	17-172 R_2 (s^{-1}) 600 MHz	17-172 NOE 600 MHz	17-144 R_1 (s^{-1}) 600 MHz	17-144 R_2 (s^{-1}) 600 MHz	17-144 NOE 600 MHz	35-172 R_1 (s^{-1}) 600 MHz	35-172 R_2 (s^{-1}) 600 MHz	35-172 NOE 600 MHz
T529	0.77 (±0.03)	2.02 (±0.04)	-0.94 (±0.01)	0.78 (±0.04)	1.70 (±0.05)	-0.88 (±0.01)			
M530	0.96 (±0.04)	2.65 (±0.03)	-0.73 (±0.01)	0.98 (±0.03)	1.97 (±0.04)	-0.75 (±0.01)			
G531	1.01 (±0.03)	2.95 (±0.06)	-0.52 (±0.03)	1.03 (±0.03)	2.29 (±0.05)	-0.51 (±0.02)			
A532	1.11 (±0.05)	3.20 (±0.05)	-0.25 (±0.02)	1.13 (±0.04)	2.78 (±0.06)	-0.23 (±0.01)			
A533	1.15 (±0.05)	4.14 (±0.08)	-0.11 (±0.01)	1.18 (±0.05)	3.42 (±0.07)	-0.09 (±0.01)			
S534	1.19 (±0.06)	4.55 (±0.08)	-0.01 (±0.01)	1.24 (±0.07)	3.74 (±0.08)	0.02 (±0.01)			
M535	1.27 (±0.04)	5.45 (±0.10)	0.23 (±0.02)	1.35 (±0.05)	4.99 (±0.09)	0.31 (±0.02)			
T536	1.30 (±0.05)	7.92 (±0.08)	0.37 (±0.01)	1.38 (±0.06)	6.41 (±0.08)	0.40 (±0.01)			
L537	1.22 (±0.06)	8.53 (±0.06)	0.57 (±0.02)	1.37 (±0.08)	7.72 (±0.07)	0.53 (±0.01)			
T538	1.24 (±0.08)	10.39 (±0.04)	0.61 (±0.02)	1.33 (±0.09)	10.00 (±0.05)	0.62 (±0.01)			
V539	1.19 (±0.06)	12.55 (±0.07)	0.68 (±0.03)	1.33 (±0.06)	9.86 (±0.08)	0.69 (±0.02)			
Q540	1.25 (±0.06)	13.38 (±0.08)	0.67 (±0.02)	1.37 (±0.06)	10.40 (±0.08)	0.67 (±0.02)			
A541	1.24 (±0.05)	13.58 (±0.09)	0.73 (±0.01)	1.34 (±0.06)	11.87 (±0.09)	0.75 (±0.01)			
R542	1.19 (±0.07)	12.70 (±0.08)	0.69 (±0.01)	1.33 (±0.07)	11.39 (±0.07)	0.71 (±0.01)			
Q543	1.22 (±0.05)	13.82 (±0.07)	0.69 (±0.02)	1.32 (±0.09)	10.95 (±0.06)	0.70 (±0.01)			
L544	1.22 (±0.06)	13.98 (±0.06)	0.71 (±0.01)	1.33 (±0.08)	10.88 (±0.06)	0.71 (±0.02)			
L545	1.18 (±0.04)	14.33 (±0.09)	0.68 (±0.02)	1.32 (±0.07)	11.12 (±0.10)	0.70 (±0.01)			
S546	1.14 (±0.06)	14.35 (±0.08)	0.68 (±0.01)	1.26 (±0.06)	11.06 (±0.09)	0.68 (±0.01)			
G547	1.21 (±0.07)	14.63 (±0.09)	0.65 (±0.01)	1.33 (±0.07)	10.69 (±0.08)	0.64 (±0.02)	0.65 (±0.04)	1.88 (±0.06)	-0.98 (±0.01)
I548	1.16 (±0.07)	14.25 (±0.09)	0.64 (±0.03)	1.28 (±0.05)	10.84 (±0.09)	0.66 (±0.03)	0.98 (±0.03)	2.60 (±0.07)	-0.40 (±0.01)
V549	1.12 (±0.08)	14.55 (±0.07)	0.66 (±0.01)	1.26 (±0.06)	11.55 (±0.08)	0.66 (±0.01)	1.13 (±0.04)	3.93 (±0.06)	-0.36 (±0.02)
Q550	1.22 (±0.09)	15.07 (±0.08)	0.60 (±0.01)	1.33 (±0.09)	10.48 (±0.07)	0.62 (±0.01)	1.20 (±0.06)	4.16 (±0.08)	-0.26 (±0.01)
Q551	1.18 (±0.08)	14.01 (±0.09)	0.63 (±0.02)	1.28 (±0.08)	9.58 (±0.08)	0.58 (±0.01)	1.28 (±0.05)	4.41 (±0.08)	-0.06 (±0.02)
Q552	1.18 (±0.09)	13.73 (±0.10)	0.56 (±0.02)	1.29 (±0.06)	10.01 (±0.10)	0.59 (±0.02)	1.34 (±0.07)	5.08 (±0.09)	0.12 (±0.02)
N553	1.16 (±0.06)	13.68 (±0.08)	0.55 (±0.02)	1.28 (±0.07)	9.69 (±0.09)	0.58 (±0.01)	1.39 (±0.06)	6.13 (±0.08)	0.32 (±0.02)
N554	1.14 (±0.07)	13.83 (±0.07)	0.62 (±0.01)	1.26 (±0.06)	10.82 (±0.07)	0.65 (±0.01)	1.37 (±0.07)	7.76 (±0.07)	0.48 (±0.01)
L555	1.12 (±0.06)	15.14 (±0.06)	0.68 (±0.02)	1.22 (±0.06)	11.26 (±0.07)	0.66 (±0.01)	1.32 (±0.06)	10.02 (±0.07)	0.61 (±0.01)
L556	1.11 (±0.09)	15.57 (±0.08)	0.69 (±0.01)	1.26 (±0.07)	11.17 (±0.08)	0.67 (±0.01)	1.29 (±0.07)	10.83 (±0.08)	0.64 (±0.02)
R557	1.15 (±0.06)	14.77 (±0.09)	0.66 (±0.02)	1.28 (±0.06)	11.20 (±0.08)	0.72 (±0.02)	1.29 (±0.07)	11.29 (±0.08)	0.68 (±0.01)
A558	1.12 (±0.10)	15.54 (±0.09)	0.68 (±0.03)	1.28 (±0.09)	11.97 (±0.09)	0.72 (±0.02)	1.34 (±0.09)	10.90 (±0.09)	0.70 (±0.02)
I559	1.10 (±0.08)	16.06 (±0.08)	0.70 (±0.01)	1.24 (±0.08)	11.77 (±0.08)	0.71 (±0.01)	1.28 (±0.08)	10.87 (±0.07)	0.68 (±0.01)
E560	1.11 (±0.09)	17.70 (±0.10)	0.70 (±0.02)	1.28 (±0.08)	12.08 (±0.09)	0.71 (±0.01)	1.29 (±0.08)	12.12 (±0.10)	0.69 (±0.01)
A561	1.14 (±0.07)	17.85 (±0.08)	0.67 (±0.01)	1.25 (±0.06)	11.83 (±0.10)	0.70 (±0.02)	1.30 (±0.07)	11.59 (±0.08)	0.68 (±0.02)
Q562	1.09 (±0.08)	17.57 (±0.09)	0.66 (±0.01)	1.21 (±0.07)	11.10 (±0.08)	0.66 (±0.01)	1.24 (±0.06)	11.02 (±0.08)	0.66 (±0.01)
Q563	1.06 (±0.09)	18.29 (±0.08)	0.68 (±0.01)	1.23 (±0.06)	11.83 (±0.09)	0.71 (±0.01)	1.21 (±0.08)	11.01 (±0.09)	0.72 (±0.02)
H564	1.13 (±0.10)	18.28 (±0.11)	0.67 (±0.01)	1.27 (±0.09)	11.14 (±0.10)	0.70 (±0.01)	1.24 (±0.09)	11.81 (±0.10)	0.71 (±0.01)
L565	1.07 (±0.08)	18.85 (±0.09)	0.68 (±0.02)	1.19 (±0.07)	11.86 (±0.09)	0.70 (±0.01)	1.17 (±0.07)	12.25 (±0.08)	0.74 (±0.01)
L566	1.10 (±0.08)	17.87 (±0.08)	0.75 (±0.01)	1.23 (±0.08)	12.48 (±0.08)	0.74 (±0.02)	1.18 (±0.08)	12.98 (±0.09)	0.77 (±0.01)
Q567	1.11 (±0.09)	17.58 (±0.09)	0.71 (±0.02)	1.17 (±0.08)	12.17 (±0.08)	0.74 (±0.01)	1.15 (±0.07)	12.49 (±0.07)	0.73 (±0.01)
L568	1.02 (±0.06)	18.02 (±0.07)	0.73 (±0.02)	1.22 (±0.06)	11.92 (±0.07)	0.71 (±0.02)	1.15 (±0.05)	13.10 (±0.06)	0.74 (±0.01)
T569	1.04 (±0.07)	17.37 (±0.05)	0.75 (±0.02)	1.21 (±0.07)	12.45 (±0.06)	0.77 (±0.01)	1.14 (±0.06)	13.03 (±0.08)	0.78 (±0.02)
V570	1.01 (±0.08)	17.19 (±0.07)	0.74 (±0.01)	1.22 (±0.09)	12.49 (±0.05)	0.76 (±0.02)	1.17 (±0.07)	13.22 (±0.06)	0.76 (±0.01)
W571	1.06 (±0.09)	16.90 (±0.09)	0.69 (±0.03)	1.23 (±0.08)	12.69 (±0.08)	0.73 (±0.02)	1.18 (±0.08)	12.46 (±0.08)	0.72 (±0.01)
G572	1.05 (±0.08)	17.25 (±0.11)	0.75 (±0.01)	1.23 (±0.06)	12.78 (±0.09)	0.77 (±0.01)	1.17 (±0.06)	13.22 (±0.09)	0.76 (±0.01)
I573	1.09 (±0.07)	17.44 (±0.09)	0.72 (±0.02)	1.28 (±0.06)	11.69 (±0.10)	0.75 (±0.02)	1.19 (±0.06)	13.35 (±0.09)	0.80 (±0.03)
K574	1.10 (±0.06)	18.05 (±0.07)	0.73 (±0.01)	1.24 (±0.07)	12.73 (±0.07)	0.78 (±0.01)	1.18 (±0.08)	12.94 (±0.07)	0.75 (±0.01)
Q575	1.07 (±0.07)	17.20 (±0.08)	0.67 (±0.01)	1.22 (±0.07)	12.26 (±0.08)	0.74 (±0.02)	1.18 (±0.08)	12.85 (±0.08)	0.76 (±0.02)
L576	1.06 (±0.05)	17.21 (±0.08)	0.70 (±0.01)	1.22 (±0.05)	12.10 (±0.08)	0.72 (±0.01)	1.18 (±0.06)	12.84 (±0.09)	0.72 (±0.01)
Q577	1.15 (±0.07)	16.65 (±0.09)	0.62 (±0.02)	1.20 (±0.07)	10.85 (±0.09)	0.70 (±0.03)	1.19 (±0.08)	13.75 (±0.08)	0.72 (±0.02)
A578	1.11 (±0.08)	15.94 (±0.06)	0.65 (±0.01)	1.25 (±0.08)	11.32 (±0.07)	0.68 (±0.01)	1.19 (±0.07)	11.95 (±0.06)	0.69 (±0.01)
R579	1.11 (±0.10)	13.95 (±0.09)	0.56 (±0.02)	1.23 (±0.09)	9.93 (±0.08)	0.61 (±0.01)	1.19 (±0.07)	10.56 (±0.08)	0.62 (±0.02)
loopS1	1.22 (±0.04)	10.39 (±0.05)	0.45 (±0.02)	1.33 (±0.05)	8.01 (±0.06)	0.52 (±0.01)	1.30 (±0.06)	8.66 (±0.05)	0.53 (±0.02)
loopG1	1.33 (±0.04)	7.27 (±0.04)	0.40 (±0.01)	1.40 (±0.04)	6.36 (±0.04)	0.45 (±0.01)	1.39 (±0.05)	6.77 (±0.05)	0.46 (±0.01)
loopG2	1.36 (±0.03)	5.70 (±0.05)	0.33 (±0.01)	1.42 (±0.03)	5.13 (±0.04)	0.37 (±0.01)	1.42 (±0.04)	5.49 (±0.04)	0.39 (±0.01)
loopR4	1.33 (±0.05)	6.02 (±0.06)	0.35 (±0.01)	1.41 (±0.04)	5.49 (±0.05)	0.38 (±0.02)	1.40 (±0.04)	5.88 (±0.04)	0.40 (±0.01)
loopG5	1.36 (±0.04)	5.54 (±0.04)	0.31 (±0.01)	1.42 (±0.05)	5.26 (±0.04)	0.37 (±0.01)	1.42 (±0.03)	5.57 (±0.05)	0.38 (±0.01)
loopG6	1.38 (±0.04)	6.98 (±0.04)	0.42 (±0.01)	1.45 (±0.04)	5.90 (±0.04)	0.44 (±0.02)	1.44 (±0.04)	6.23 (±0.04)	0.46 (±0.02)
W628	1.24 (±0.08)	11.95 (±0.08)	0.52 (±0.01)	1.38 (±0.08)	8.96 (±0.08)	0.59 (±0.02)	1.41 (±0.04)	10.88 (±0.07)	0.59 (±0.01)
M629	1.24 (±0.08)	14.66 (±0.09)	0.62 (±0.02)	1.37 (±0.06)	10.27 (±0.08)	0.65 (±0.01)	1.33 (±0.08)	11.52 (±0.08)	0.63 (±0.02)

E630	1.16 (±0.09)	14.31 (±0.09)	0.65 (±0.01)	1.32 (±0.09)	9.48 (±0.09)	0.65 (±0.01)	1.26 (±0.09)	11.03 (±0.11)	0.68 (±0.01)
W631	1.16 (±0.10)	14.82 (±0.11)	0.65 (±0.01)	1.33 (±0.08)	10.53 (±0.10)	0.66 (±0.02)	1.27 (±0.08)	11.15 (±0.08)	0.67 (±0.02)
D632	1.11 (±0.08)	16.52 (±0.10)	0.69 (±0.02)	1.29 (±0.08)	11.39 (±0.09)	0.72 (±0.01)	1.23 (±0.09)	12.06 (±0.08)	0.69 (±0.01)
R633	1.10 (±0.07)	16.90 (±0.09)	0.64 (±0.01)	1.26 (±0.06)	12.00 (±0.08)	0.65 (±0.01)	1.25 (±0.08)	11.31 (±0.09)	0.68 (±0.01)
E634	1.12 (±0.07)	16.81 (±0.08)	0.63 (±0.01)	1.29 (±0.07)	10.77 (±0.08)	0.66 (±0.01)	1.24 (±0.07)	11.76 (±0.08)	0.69 (±0.01)
I635	1.11 (±0.06)	16.28 (±0.07)	0.66 (±0.01)	1.28 (±0.07)	11.46 (±0.07)	0.71 (±0.01)	1.21 (±0.07)	12.02 (±0.06)	0.72 (±0.02)
N636	1.10 (±0.08)	17.06 (±0.08)	0.67 (±0.01)	1.29 (±0.06)	11.10 (±0.08)	0.70 (±0.02)	1.23 (±0.06)	12.34 (±0.08)	0.70 (±0.01)
N637	1.07 (±0.09)	17.11 (±0.07)	0.68 (±0.01)	1.27 (±0.09)	10.89 (±0.07)	0.67 (±0.01)	1.22 (±0.09)	11.84 (±0.08)	0.70 (±0.02)
Y638	1.11 (±0.06)	16.96 (±0.08)	0.67 (±0.02)	1.31 (±0.07)	11.29 (±0.07)	0.66 (±0.03)	1.24 (±0.08)	11.42 (±0.07)	0.68 (±0.03)
T639	1.05 (±0.05)	17.46 (±0.08)	0.69 (±0.01)	1.26 (±0.06)	11.51 (±0.08)	0.73 (±0.01)	1.18 (±0.06)	12.75 (±0.07)	0.73 (±0.02)
S640	1.09 (±0.07)	16.92 (±0.09)	0.71 (±0.01)	1.28 (±0.07)	11.58 (±0.08)	0.74 (±0.01)	1.17 (±0.06)	12.36 (±0.08)	0.71 (±0.01)
L641	1.07 (±0.08)	18.12 (±0.10)	0.70 (±0.02)	1.29 (±0.06)	11.72 (±0.09)	0.72 (±0.01)	1.20 (±0.07)	12.79 (±0.09)	0.73 (±0.01)
I642	1.13 (±0.09)	16.95 (±0.06)	0.68 (±0.03)	1.33 (±0.09)	10.70 (±0.05)	0.72 (±0.02)	1.18 (±0.08)	12.99 (±0.06)	0.70 (±0.01)
H643	1.10 (±0.09)	17.32 (±0.07)	0.73 (±0.01)	1.33 (±0.08)	11.22 (±0.07)	0.73 (±0.01)	1.23 (±0.09)	12.60 (±0.07)	0.75 (±0.02)
S644	1.06 (±0.06)	17.35 (±0.08)	0.72 (±0.01)	1.29 (±0.05)	11.02 (±0.08)	0.72 (±0.01)	1.20 (±0.05)	12.58 (±0.08)	0.75 (±0.01)
L645	1.09 (±0.08)	17.68 (±0.09)	0.72 (±0.01)	1.34 (±0.07)	11.27 (±0.09)	0.70 (±0.02)	1.22 (±0.06)	12.67 (±0.08)	0.72 (±0.01)
I646	1.10 (±0.09)	18.09 (±0.09)	0.70 (±0.02)	1.35 (±0.08)	10.71 (±0.09)	0.69 (±0.01)	1.22 (±0.07)	13.03 (±0.09)	0.69 (±0.02)
E647	1.13 (±0.10)	16.38 (±0.06)	0.63 (±0.01)	1.35 (±0.09)	10.38 (±0.08)	0.64 (±0.01)	1.24 (±0.06)	12.35 (±0.08)	0.70 (±0.01)
E648	1.13 (±0.06)	15.80 (±0.07)	0.57 (±0.02)	1.38 (±0.06)	8.86 (±0.07)	0.56 (±0.01)	1.22 (±0.08)	10.92 (±0.06)	0.64 (±0.02)
S649	1.17 (±0.06)	14.97 (±0.08)	0.52 (±0.01)	1.39 (±0.06)	7.41 (±0.08)	0.45 (±0.02)	1.27 (±0.08)	10.02 (±0.08)	0.59 (±0.01)
Q650	1.17 (±0.08)	13.13 (±0.09)	0.52 (±0.02)	1.41 (±0.07)	6.28 (±0.09)	0.33 (±0.01)	1.30 (±0.07)	9.90 (±0.09)	0.57 (±0.01)
N651	1.18 (±0.07)	12.87 (±0.08)	0.49 (±0.02)	1.38 (±0.06)	4.36 (±0.08)	0.14 (±0.01)	1.28 (±0.05)	9.08 (±0.08)	0.55 (±0.02)
Q652	1.19 (±0.08)	12.19 (±0.09)	0.46 (±0.02)	1.32 (±0.06)	2.76 (±0.08)	-0.12 (±0.02)	1.32 (±0.06)	7.40 (±0.09)	0.46 (±0.02)
Q653	1.25 (±0.07)	11.80 (±0.06)	0.39 (±0.01)	1.23 (±0.07)	2.09 (±0.06)	-0.38 (±0.01)	1.34 (±0.06)	8.02 (±0.08)	0.46 (±0.01)
E654	1.25 (±0.09)	12.50 (±0.12)	0.43 (±0.03)	1.08 (±0.05)	1.62 (±0.06)	-0.69 (±0.01)	1.34 (±0.07)	8.53 (±0.11)	0.48 (±0.02)
K655	1.23 (±0.05)	12.31 (±0.05)	0.43 (±0.01)	0.84 (±0.04)	1.14 (±0.05)	-1.18 (±0.01)	1.34 (±0.05)	8.65 (±0.06)	0.52 (±0.01)
N656									
E657	1.20 (±0.07)	12.80 (±0.06)	0.51 (±0.01)				1.30 (±0.07)	9.82 (±0.07)	0.56 (±0.01)
Q658	1.18 (±0.08)	13.64 (±0.07)	0.51 (±0.01)				1.29 (±0.08)	9.33 (±0.07)	0.60 (±0.02)
E659	1.18 (±0.09)	14.31 (±0.08)	0.61 (±0.02)				1.29 (±0.08)	10.77 (±0.08)	0.63 (±0.01)
L660	1.18 (±0.10)	15.18 (±0.09)	0.61 (±0.03)				1.30 (±0.09)	11.33 (±0.10)	0.63 (±0.03)
L661	1.15 (±0.07)	15.97 (±0.06)	0.67 (±0.01)				1.26 (±0.07)	10.94 (±0.07)	0.65 (±0.01)
E662	1.17 (±0.07)	14.91 (±0.08)	0.64 (±0.01)				1.27 (±0.06)	11.54 (±0.08)	0.66 (±0.02)
L663	1.14 (±0.09)	15.58 (±0.12)	0.70 (±0.01)				1.29 (±0.08)	11.37 (±0.09)	0.62 (±0.01)
D664	1.13 (±0.06)	15.96 (±0.08)	0.65 (±0.01)				1.25 (±0.05)	11.76 (±0.08)	0.68 (±0.01)
K665	1.14 (±0.08)	15.95 (±0.09)	0.65 (±0.02)				1.27 (±0.06)	11.49 (±0.08)	0.69 (±0.01)
W666	1.14 (±0.09)	15.10 (±0.10)	0.65 (±0.01)				1.25 (±0.08)	11.57 (±0.09)	0.68 (±0.02)
A667	1.13 (±0.07)	16.05 (±0.09)	0.70 (±0.01)				1.24 (±0.07)	12.10 (±0.07)	0.69 (±0.01)
S668	1.09 (±0.06)	16.55 (±0.08)	0.68 (±0.01)				1.21 (±0.06)	12.98 (±0.08)	0.68 (±0.02)
L669	1.18 (±0.06)	15.62 (±0.07)	0.66 (±0.01)				1.28 (±0.06)	13.22 (±0.08)	0.67 (±0.01)
W670	1.14 (±0.07)	16.25 (±0.08)	0.60 (±0.02)				1.26 (±0.07)	13.07 (±0.08)	0.71 (±0.02)
N671	1.13 (±0.08)	17.84 (±0.08)	0.63 (±0.01)				1.25 (±0.08)	14.32 (±0.07)	0.67 (±0.02)
W672	1.12 (±0.08)	17.95 (±0.09)	0.64 (±0.01)				1.24 (±0.06)	14.28 (±0.09)	0.65 (±0.02)
F673	1.17 (±0.06)	17.90 (±0.06)	0.66 (±0.02)				1.28 (±0.07)	14.19 (±0.06)	0.72 (±0.01)
N674	1.19 (±0.07)	17.36 (±0.07)	0.63 (±0.01)				1.31 (±0.06)	13.95 (±0.08)	0.64 (±0.01)
I675	1.17 (±0.05)	16.86 (±0.06)	0.61 (±0.01)				1.27 (±0.05)	12.93 (±0.07)	0.64 (±0.02)
T676	1.21 (±0.06)	14.62 (±0.08)	0.71 (±0.02)				1.32 (±0.06)	12.23 (±0.07)	0.70 (±0.01)
N677	1.20 (±0.08)	13.91 (±0.08)	0.68 (±0.01)				1.31 (±0.08)	11.94 (±0.08)	0.68 (±0.02)
W678	1.20 (±0.06)	13.87 (±0.09)	0.65 (±0.01)				1.32 (±0.07)	10.82 (±0.10)	0.64 (±0.01)
L679	1.22 (±0.07)	14.42 (±0.06)	0.65 (±0.01)				1.34 (±0.07)	9.58 (±0.06)	0.65 (±0.02)
W680	1.25 (±0.06)	13.60 (±0.05)	0.65 (±0.02)				1.38 (±0.06)	10.52 (±0.06)	0.66 (±0.01)
Y681	1.26 (±0.05)	13.94 (±0.06)	0.62 (±0.01)				1.40 (±0.05)	9.84 (±0.05)	0.62 (±0.01)
I682	1.34 (±0.05)	11.67 (±0.06)	0.54 (±0.01)				1.42 (±0.06)	9.71 (±0.05)	0.56 (±0.01)
K683	1.38 (±0.03)	11.98 (±0.04)	0.43 (±0.01)				1.43 (±0.04)	8.02 (±0.06)	0.43 (±0.01)

The six residues replacing the immunodominant loop (I69-T116) in the Core^S constructs are numbered loopS1-loopG6

References

- Bohm, G, Muhr, R, Jaenicke, R (1992) Quantitative analysis of protein far UV circular dichroism spectra by neural networks. *Protein Eng* 5: 191-195.
- Cole, JL, Lary, JW, Moody, TP, Laue, TM (2008). Analytical ultracentrifugation: Sedimentation velocity and sedimentation equilibrium. *Biophysical Tools for Biologists: Vol 1 in Vitro Techniques*. **84**: 143-179.
- Ghirlando, R, Balbo, A, Piszczek, G, Brown, PH, Lewis, MS, Brautigam, CA, Schuck, P, Zhao, H (2013) Improving the thermal, radial, and temporal accuracy of the analytical ultracentrifuge through external references. *Anal Biochem* 440: 81-95.
- Inagaki, S, Ghirlando, R, Grisshammer, R (2013) Biophysical characterization of membrane proteins in nanodiscs. *Methods* 59: 287-300.
- le Maire, M, Champeil, P, Moller, JV (2000) Interaction of membrane proteins and lipids with solubilizing detergents. *Biochimica Et Biophysica Acta-Biomembranes* 1508: 86-111.
- Schuck, P (2000) Size-distribution analysis of macromolecules by sedimentation velocity ultracentrifugation and Lamm equation modeling. *Biophys J* 78: 1606-1619.
- Zhao, H, Brautigam, CA, Ghirlando, R, Schuck, P (2013) Overview of current methods in sedimentation velocity and sedimentation equilibrium analytical ultracentrifugation. *Current protocols in protein science / editorial board, John E Coligan [et al] Chapter 20: Unit20.12-Unit20.12.*
- Zhao, H, Brown, PH, Schuck, P (2011) On the Distribution of Protein Refractive Index Increments. *Biophys J* 100: 2309-2317.